Semicond. Sci. Technol. **12** (1997) 1046–1051. Printed in the UK PII: S0268-1242(97)80860-7

Fabrication of quantum wires in thermally etched V-grooves by molecular beam epitaxy

D Scheiner†, Y Hanein and M Heiblum

Braun Center for Submicron Research, Department of Condensed Matter Physics, Weizmann Institute of Science, Rehovot 76100, Israel

Received 10 January 1997, accepted for publication 7 May 1997

Abstract. Quasi-one-dimensional quantum wires have been formed in V-grooves on GaAs substrates. A new fabrication technique based on *in situ* thermal etching of masked substrates and subsequent overgrowth by molecular beam epitaxy has been developed. The device geometries enabled formation of low-resistance ohmic contacts. Two-terminal magnetoresistance measurements of single-wire devices show transport qualities previously not witnessed in growth on non-planar substrates. Illumination has been used to modulate the carrier density and lateral potential profile of the wires.

Fabrication techniques based on the formation of quantum wells (QW) with additional lateral bandgap confinement are expected to form true one-dimensional (1D) quantum wires. Formation of such wires by direct epitaxial growth on prepatterned substrates is a promising technique. Indeed, fabrication by metal-organic chemical vapour deposition (MOCVD) on substrates with prepatterned V-shaped grooves has lead to very narrow wires with lateral heterojunction confinement [1]. Limitations of material quality, though, have not permitted reliable conductance measurements and experiments have concentrated on the optical properties of such structures. However, the wires' optical qualities were sufficiently good to make quantum wire laser diodes with much future potential [2].

The most successful realization to date of 1D devices suited for transport measurements, was that made by cleaved edge overgrowth using molecular beam epitaxy (MBE) [3, 6]. Magnetoresistance measurements [4, 5] and quantized conductance [6] effects were measured. Another technique used etching of very high-mobility modulation-doped-heterostructures [7] and evaporated side gates to achieve quantized conductance.

In this paper we report on the fabrication and characterization of quasi-one-dimensional (1D) quantum wires grown in $(01\bar{1})$ V-grooves with (111)A slopes, using MBE. Previous reports on MBE-grown wires in grooves were only of their photoluminescence properties [8, 9]. Growth in grooves made in the (011) direction, with (111)B slopes, showed confinement due to the formation of crescent-shaped constrictions at the bottom tip [9]. Our technique is based on an *in situ* process of thermally etched V-grooves [10], employing a mask material compatible with the MBE process, and utilizing novel groove geometries. The technique enables growth on grooves in the $(01\bar{1})$ direction, with (111)A slopes which form a 70° corner at the bottom, as well as on unique grooves formed along the (001) diagonal, with (110) slopes which form a 90° corner. The kinetics of the MBE growth on the $(01\bar{1})$ grooves' slopes enables formation of narrow wires of controlled width, on the (001) plane, formed at the bottom of the grooves. Such a structure was not achieved before in a smooth and continuous form because of the unstable growth on (111)A planes.

The initial epitaxial growth consists of a 3 μm thick GaAs buffer layer, a 1000 Å thick $Al_{0.3}Ga_{0.7}As$ masking layer and a 1000 Å thick GaAs cap layer. The two top layers are wet etched, after a lithography step, to form an extremely clean and stable mask. After careful cleaning, the patterned wafer is loaded into a thermal processing chamber and heated to a high temperature ($\sim$710 °C) under an impinging arsenic flux of about 5×10^{-6} Torr, thereby undergoing thermal etching (sublimation) of the GaAs unprotected by the AlGaAs mask. It is surmised that the mask layer remains stable due to the formation of a thin impenetrable AlAs coating after the initial stages of thermal etching. The etch rate of GaAs in the (100) direction in wide areas is about 3000 Å h^{-1} under these conditions. Extremely smooth and sharp V-shaped grooves are formed in the narrow gaps in the mask, aligned to predetermined crystallographic directions (see figure 1). In narrow grooves the thermal etch rate is somewhat higher due to arsenic flux shadowing. After the V-shaped profile is attained, the effective vertical etch rate drops by almost an order of magnitude. To enhance the purity of the groove surface, the thermal etching is carried out within the thick epitaxial buffer layer and not into the substrate material. After etching, the wafer is transferred *in situ* into

† Present address: Nova Measuring Instruments Ltd, Weizmann Science Park, Rehovot 76100, Israel (e-mail address: david-s@nova.co.il).

0268-1242/97/081046+06$19.50

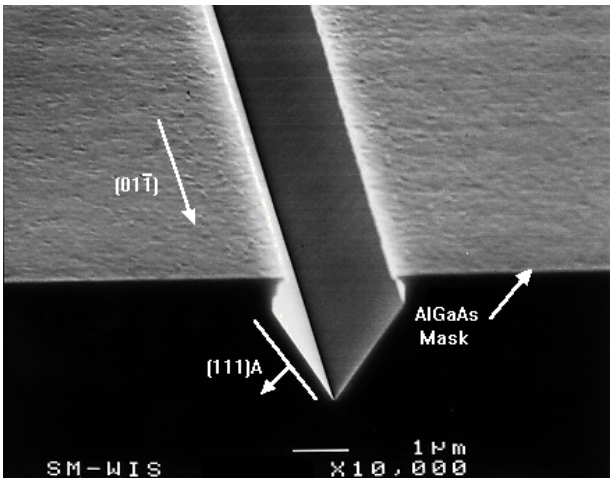

Figure 1. Thermal etching of a long V-groove in the (01$\bar{1}$) direction. The 1000 Å thick AlGaAs mask is slightly roughened during the thermal etching. Short vertical (011) planes are visible under the mask above the (111)A slopes. The bottom of the V-groove is extremely straight irrespective of roughness of the edge of the mask.

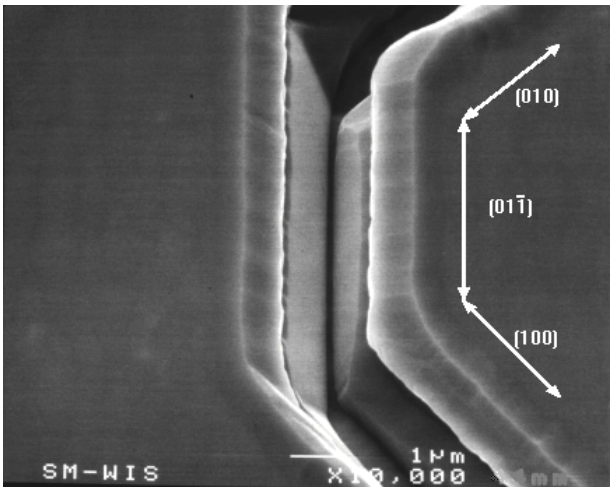

Figure 2. 7 μm long quantum wire groove integrated with diagonal grooves. Note the extremely smooth surface on the groove slopes and the micron long funnels formed by the epitaxial growth at the meeting of the wire and the diagonal grooves.

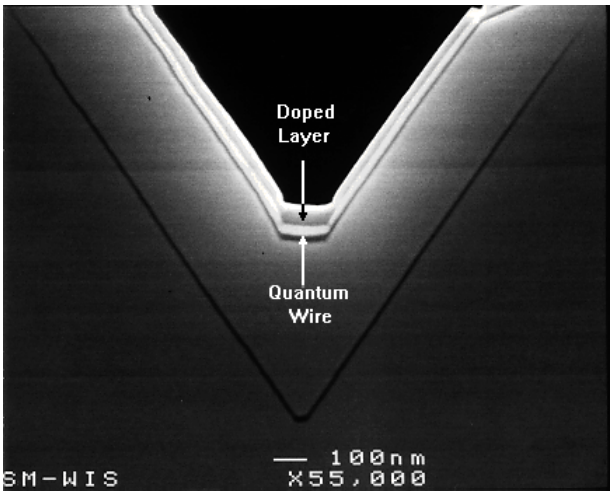

Figure 3. Differentially stained cross-section of epitaxial growth in a V-groove. Darker layers are AlGaAs, the quantum wire layer is the bright bar about 700 Å below the surface. The thickness of the growth on the slopes is about 60% of that at the bottom.

the MBE growth chamber and a GaAs–AlGaAs modulation doped structure is grown on it. The growth is problematic because of the instability of the growth on the (111)A slopes and *shadowing* effects in the groove. Smooth growth on (111)A planes requires high arsenic flux and low substrate temperatures. Additionally, flux coverage of the groove slopes suffers from cyclic shadowing problems due to the rotation of the substrate under the oblique angle of the incoming arsenic flux. This problem is dealt with by maintaining a total V/III beam equivalent flux ratio of over 100 from two widely spaced arsenic sources and using a high substrate rotation frequency (two cycles per nominal monolayer), thus ensuring smooth growth. The nominal total arsenic beam equivalent pressure is about 1.2×10^{-5} Torr.

Alloying ohmic contacts directly to the narrow wires in the grooves results in a high contact resistance ($\sim$100 kΩ at 4 K after illumination), as is already known [11]. This makes measurements difficult, since four-terminal measurement configurations are not possible. We have utilized the unique qualities of the thermal etching process to integrate the quantum wires in series with the diagonal (001) grooves (see figure 2). This type of groove cannot be formed by anisotropic *wet etching* techniques because the non-polar (110) slopes do not stabilize during wet etching. The large diffusion length of gallium atoms on (110) slopes inhibits growth on them and a relatively wide epitaxial plane is formed at the bottom of such grooves. For a total nominal growth thickness of 0.4 μm on the (100) plane, the width of the nearly flat bottom is about 1 μm while the width of the wires is about 1000 Å. Additionally, longitudinal surface diffusion of gallium along the grooves, of the order of a micron, causes formation of a smooth funnel-like transition region from the wide-bottom *diagonal* grooves to the narrow-bottom quantum wire grooves (see figure 2).

The epitaxial growth consists of a layer sequence similar to that used for conventional modulation doped two-dimensional electron gas (2DEG) structures. The main differences consist of enhanced silicon doping to overcome shadowing effects in the groove and an additional AlGaAs barrier below the electron gas to form a quantum well (QW), thus confining the electrons in both wire and groove slopes. Since the QW width on the slopes is markedly thinner than that on the (100) plane (see figure 3), the energy of the eigenstates there is higher, forming an effective energy barrier. The typical layer sequence from the substrate up is as follows: 50 Å $Al_{0.4}Ga_{0.6}As$ marker, 2500 Å undoped GaAs buffer, 400 Å $Al_{0.4}Ga_{0.6}As$ barrier, 300 Å GaAs QW, 200 Å $Al_{0.4}Ga_{0.6}As$ undoped spacer, 200 Å $Al_{0.4}Ga_{0.6}As$ Si-doped layer (3×10^{18} cm^{-3}), 100 Å

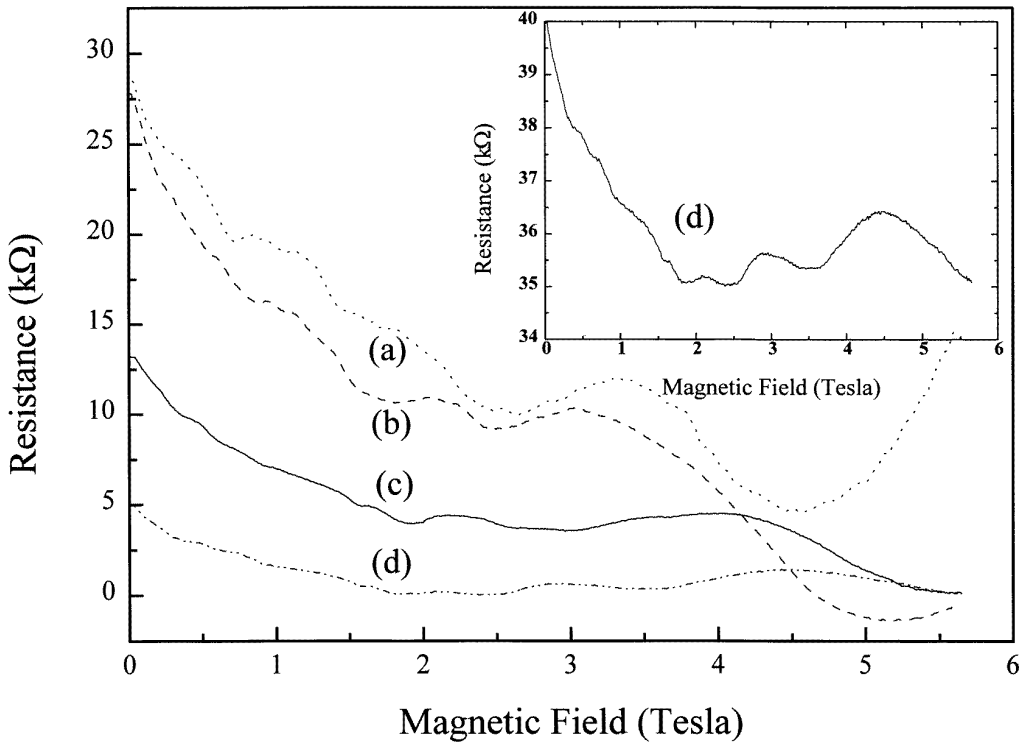

Figure 4. Shubnikov–de Haas magnetoresistance curves of a 6 μm long wire from sample with strongly p-doped slopes after different illumination levels. Curves have been arbitrarily offset for clarity: (a) $R(B = 0) = 132$ kΩ (104 kΩ subtracted); (b) $R(B = 0) = 94$ kΩ (66 kΩ subtracted); (c) $R(B = 0) = 53$ kΩ (40 kΩ subtracted); and (d) $R(B = 0) = 40$ kΩ (35 kΩ subtracted). The inset shows the strongly illuminated case before subtraction. Note the strong negative magnetoresistance up to 1.8 T and the onset of strong SdH oscillations at a similar field.

$Al_{0.4}Ga_{0.6}As$ layer, 250 Å GaAs cap. The thicknesses are for growth on (100). The growth temperature of the buffer layer grown below the AlGaAs barrier determines the width of the quantum wire: the higher the temperature, the more diffusion from the slopes, the wider the wire. To achieve geometrical wire widths of ∼1000 Å, a substrate temperature of about 570 °C is maintained under the above mentioned As pressure. Changes in substrate temperature of ±30 °C result in width variations of ±20%. Varying the As pressure also affects the width. Silicon is an amphoteric dopant, i.e. it can be either a p-dopant (on As lattice sites) or an n-dopant (on Ga sites) [12, 13]. In the present structure p-type slopes aid in the lateral confinement of carriers to the 1D region by formation of an additional potential barrier that prevents the electrons in the wire from flowing into the QW on the slopes [14]. Hence, the growth temperature during the deposition of the doped layer is an effective degree of freedom for tuning the active p-doping density and thus the effective width and electron density in the wire.

Low-resistance ohmic contacts are formed, in turn, by evaporating Au/Ge/Ni contacts overlapping the diagonal grooves. Although the epitaxial growth on the mesas outside the grooves forms a conducting 2DEG that is also contacted, the undercut profile formed during the thermal etching prevents continuity and current by-passing the wire over the top of the mesas. To estimate the contact resistance in the diagonal grooves we measured the resistance between two contacts placed 5 μm apart on the same wide diagonal groove. Prior to illumination the resistance is found to be in the range 6–14 kΩ at 4.2 K. After illumination this resistance decreased in some cases to about 2 K. Shubnikov–de Haas (SdH) magnetoresistance measurements of the *diagonal* leads show no oscillations in magnetic field, only a strong positive magnetoresistance at high fields. This is most probably due to the low mobility resulting from the rough morphology in the *diagonal* grooves. The resistance of the funnel transition regions is not insignificant; even in short devices in which the wire is washed out due to merging of the two funnels, the minimum resistance is still at least 10 kΩ.

Two-terminal SdH measurements have been performed at liquid helium temperatures on single-wire devices from a number of different samples. By controlling the substrate temperature during growth of the doped layer, three types of doping methods were employed; all produced wires which were highly resistive when cooled to 4.2 K in the dark. First, silicon doping was performed at low substrate temperature of about 570 °C and/or high arsenic flux $>1.5 \times 10^{-5}$ Torr. After illumination by an infrared GaAs light emitting diode (with a spectral energy tail above the bandgap) the devices exhibited n-type conduction on the slopes of the grooves which effectively short-circuited the wires. This could be seen from SdH measurements with the magnetic field parallel to the wafer surface with a component perpendicular only to the slopes. Second, we attempted to form heavily p-doped slopes. This was achieved when the silicon doping was performed at high

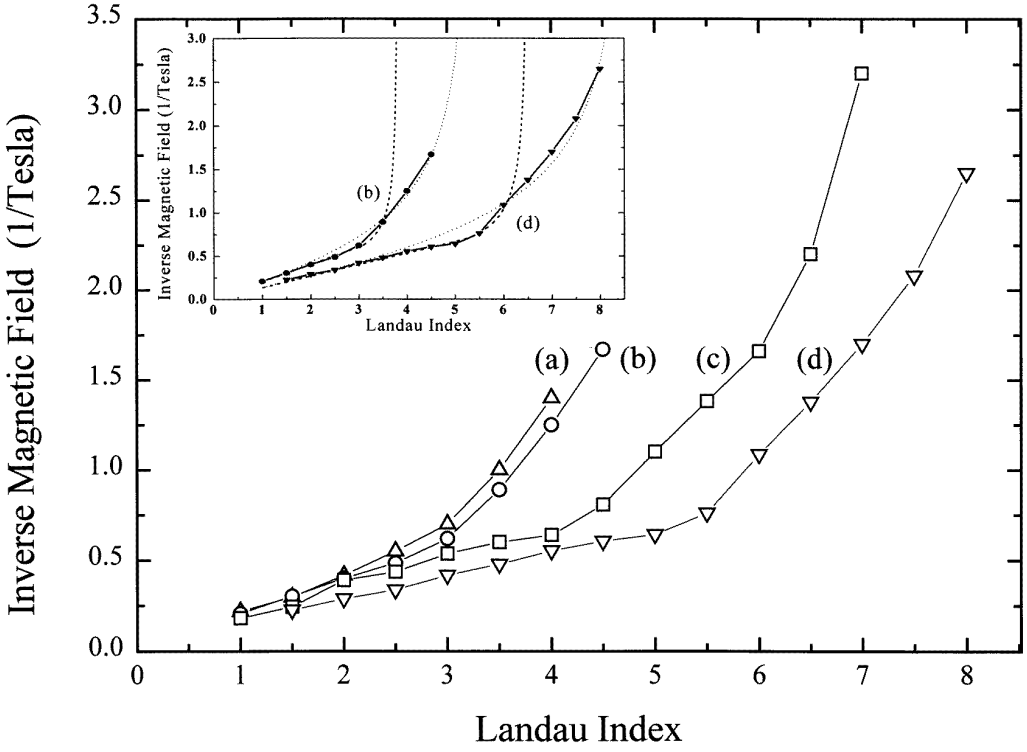

Figure 5. Landau plots of 6 μm long quantum wire from sample with strongly p-doped slopes. Curves show measurements after different levels of illumination. The carrier concentrations deduced from the slope of the plots at low Landau level index are: (a) $R(B = 0) = 132$ kΩ, $n = 2.3 \times 10^{11}$ cm^{-2}; (b) $R(B = 0) = 94$ kΩ, $n = 2.4 \times 10^{11}$ cm^{-2}; (c) $R(B = 0) = 53$ kΩ, $n = 3.0 \times 10^{11}$ cm^{-2}; and (d) $R(B = 0) = 40$ kΩ, $n = 3.9 \times 10^{11}$ cm^{-2}. The inset shows parabolic (dotted curves) and square-well (broken curves) fits for curve (b) with $W_{par} = 1800$ Å and $W_{sq} = 950$ Å respectively. Similarly the parabolic and square-well fits for curve (d) are $W_{par} = 2200$ Å and $W_{sq} = 1250$ Å respectively.

substrate temperatures exceeding 630 °C. Upon illumination the wires became conducting but the conductance dropped drastically when the light was turned off. This suggests that the wires were depleted from both slopes at equilibrium, but that the light-generated carrier pairs, that were spatially separated by the built-in field of the lateral p–n–p structure, enabled conduction. The generated carriers sharpened the potential well formed by the p–n–p band bending, with electrons filling the conduction band 'pocket' and holes flowing up the slopes. Upon terminating the illumination, carriers underwent spatially indirect recombination and the strong p-doping of the slopes led to a depletion of the wires. Third, by growing the doped layer at a substrate temperature of ∼600 °C and arsenic pressure of 1.2×10^{-5} Torr, we attempted to create only weakly p-doped or compensated slopes enabling conduction in the wires, but without *parallel conduction* on the slopes. Indeed, we found persistent photoconductivity after illumination since the weakly p-doped slopes were not capable of completely emptying the electrons from the wires. For such wires, SdH measurements gave high electron concentrations and an estimated effective width similar to that of the geometrical one. Meaningful measurements were achieved on a number of samples from different growth runs.

Information on the lateral confining potential can be obtained by displaying the SdH measurements as Landau plots, i.e. the inverse magnetic field values of the extrema of the SdH oscillations versus Landau level index [15]. For a 2DEG the Landau plots should be straight lines (i.e. linear magnetic depopulation) with slope dependent on carrier concentration, while for a lateral confining potential a deviation from linearity is expected depending on the potential shape. The plot for a parabolic confinement profile $V(x) = \frac{1}{2}m\omega_0^2 x^2$, with width $W_{par} = 2\overline{h}k_f/m\omega_0$ (W_{par} is obtained from the semiclassical turning points at the Fermi energy $E_f = \frac{1}{2}m\omega_0^2(\frac{1}{2}W_{par})^2$) gives the SdH resistance minima of the resulting hybrid electromagnetic subbands at the values [15]

$$N_{par} = \mathrm{Int}\left\{\frac{1}{2} + \frac{1}{4}K_f W_{par}\left[1 + \left(\frac{W_{par}}{2\ell_c}\right)^2\right]^{-1/2}\right\} \quad (1)$$

with $\ell_c = \overline{h}k_f/eB$ the cyclotron radius of electrons at the Fermi energy. This describes a continuous deviation of the Landau plot from linearity starting at low values of inverse magnetic field. Similarly for a square-well confinement potential of infinite depth and width of W_{sq}, a semiclassical approximation gives the resistance minima at the values [15]

$$N_{sq} \simeq \mathrm{Int}\left\{\frac{2}{\pi}\frac{E_f}{\overline{h}\omega_c}\left[\arcsin\left(\frac{W_{sq}}{2\ell_c}\right) + \frac{W_{sq}}{2\ell_c}\sqrt{1 - \left(\frac{W_{sq}}{2\ell_c}\right)^2}\right]\right\} \pm 1 \quad (2)$$

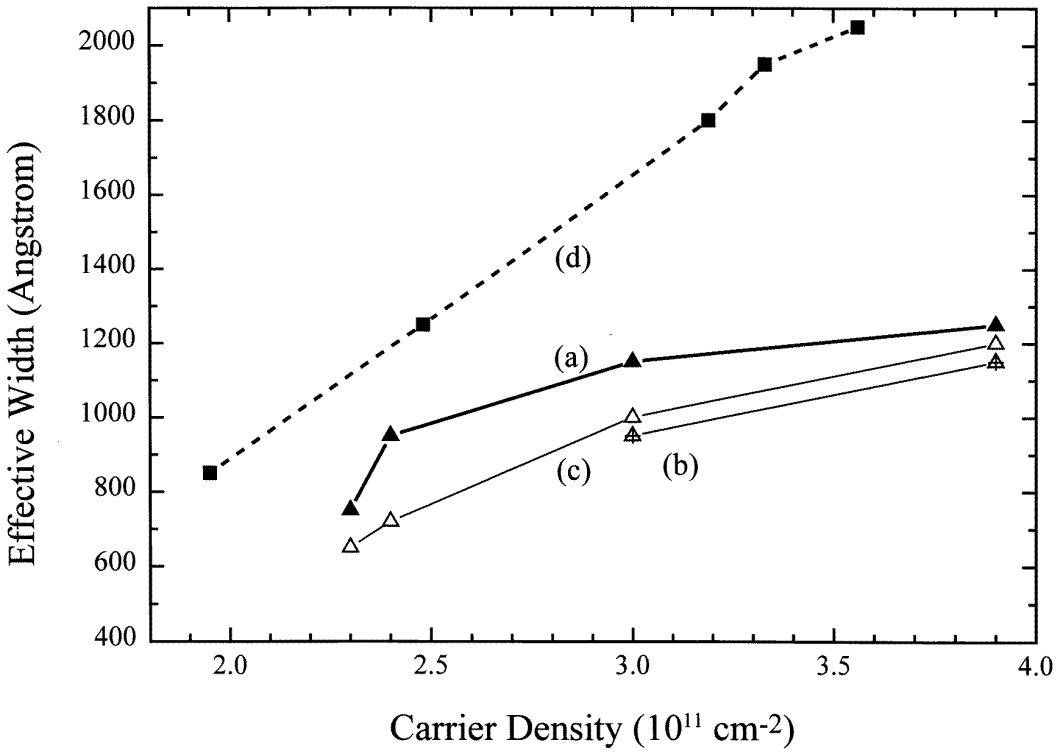

Figure 6. Effective width versus electron density for two samples with 300 Å QW. The electron density is modulated by illumination. The width estimates for the strong p-doping sample are from: (a) width of square-well potential to fit turning point in Landau plots; (b) saturation of negative magnetoresistance in SdH data; (c) onset of strong SdH oscillations. For the weak p-doping sample: (d) width of square-well potential to fit turning point in Landau plots. Plots (a) and (d) show different modes of lateral confinement. The sample with weaker p-doping on the slopes (d) gives a wide, non-saturating effective width while the strongly doped sample gives a saturation at the geometrical width (a).

for low fields with $2\ell_c > W_{sq}$. For high magnetic fields the result merges with the 2DEG result

$$N_{2D} \simeq \mathrm{Int}\left(\frac{1}{2} + \frac{E_f}{\hbar\omega_c}\right). \tag{3}$$

This gives a sharp deviation from the linear relation and the turning point provides an indication of the width of the channel.

Typical results were obtained on wires of typical geometrical widths of 1200 Å (measured in a scanning electron microscope). Grooves with various lengths in the $(01\bar{1})$ direction became conductive after illumination. Upon terminating the illumination the resistance rose by a factor of 2 to 3 over a period of about an hour. The electrons were confined in a 300 Å thick QW while the slopes had a QW some 170 Å thick. The well thickness on the slopes is relatively wide, confinement is mostly via p–n junctions between the bottom (100) and the slopes. Measurements were performed in the dark after several cycles of illumination, with resistance stabilizing at successively lower values each time. Due to the spatial separation of electrons and holes, the quasi steady state potential enables electron densities in the wires double that of the equilibrium value in flat 2DEG regions. No SdH oscillations were observed in a magnetic field parallel to the surface with a component normal only to the slopes, indicating that the slopes were not n-type.

Figure 4 shows four SdH measurements of a 6 μm long wire after successive illumination cycles, offset for clarity by large resistances (see figure caption). The Landau plots of the resistance extrema appearing in figure 5 are obtained after subtracting a parabolic fit to the SdH data of figure 4 at low magnetic fields. In all cases, (see figure 5 curves (a)–(d)) the Landau plots deviate from linearity and can be well fitted at high Landau index, i.e. low fields, using a parabolic confinement profile with a width $W_{par} \simeq$ 2000 Å (shown for (b) and (d) in the inset of figure 5). At lower filling factors the curve can be fitted (demonstrated for (b) and (d) in the inset of figure 5) using the predicted depopulation in an infinite square-well potential with widths between 750 Å (a) and 1250 Å (d), and electron concentrations between 2.3×10^{11} cm^{-2} and 3.9×10^{11} cm^{-2} respectively. For the other curves in figure 5, fitting to intermediate potentials, between parabolic and square-well confinements, also appears appropriate. We assume therefore that the carrier density is sufficiently high in all the cases to flatten the potential at the centre of the wire while the p–n junctions at the edges bend the potential. Taking into account the series resistance and the geometry of the wire, for the lowest resistance case the mobility is found to be approximately 160 000 cm^2 V^{-1} s^{-1} with an elastic mean free path of about 1.6 μm.

Curve (a) in figure 6 is a summary of the results of the analysis of the SdH measurements done with the 6 μm

long wire. It shows the increase of the estimated wire width as carrier density increases and resistance drops from 132 kΩ to 40 kΩ. The widest electrical width is estimated to be 1250 Å, close to the geometrical width of the wire. One can also estimate the width directly from the low-field magnetoresistance (see, for example, the inset in figure 4) [15]. It has a sharp drop in the resistance with magnetic field, saturating at $\ell_c \simeq 0.5W$. The field values at which the negative magnetoresistance diminishes is discernible in the SdH curves (c) and (d) in figure 4 and its corresponding channel width is shown figure 6 curve (b). A third method to estimate the wire width is to follow the SdH oscillation amplitude. One observes a sharp increase in the oscillation amplitude (see inset in figure 4) at some magnetic field ascribed to the confinement of the electron orbits to the bottom of the groove with wavefunction with small overlap with the rougher slopes. The cyclotron diameter associated with such transitions, somewhat smaller than those deduced from the Landau plots, are shown in figure 6 curve (c). We have found that for this sample the three different estimates provide roughly similar channel widths.

Qualitatively, transformation from a weakly confined parabolic shape to a wide flat bottomed potential, as the carrier density increases, was seen in numerical modelling of a very similar V-groove structure [14]. In that report, the minimum width that enabled a flat potential to develop in the centre of the groove was of the order of 1000 Å.

Similar measurements were performed on another sample with a narrower geometrical width, 1000 Å, and a length of 5 μm. Successive illuminations did not lead to saturation at the electrical width; instead, the effective width, inferred from the Landau plots, rose monotonically (figure 6 curve (d)). The two other methods of determining the width of this wire (not shown in figure 6) *do* exhibit saturation at the geometrical width similar to curves (b) and (c) in figure 6. The non-saturating electrical width obtained from the Landau plots is consistent with a weak lateral confinement caused by a lightly doped p-region and a severe flattening of the potential at the centre of the wire by the high electron density. The narrower widths obtained from the other estimates might be attributed to the rough potential barrier induced by the slopes due to inhomogeneous AlGaAs growth there. Thus the limiting size for negative magnetoresistance and strong oscillations remains the width of the groove bottom even when the electrical width is larger.

Measurements were also performed on a sample with carriers confined to a 100 Å QW and geometrical width 1300 Å. The *turning points* in the Landau plots for all carrier densities gave a single width, 1250 Å; an indication that even though the slopes are only weakly p-doped the electrons are confined to the bottom due to the narrow 60 Å wide QW on the slopes. This is in contrast to the previous samples with a 300 Å thick QW, where measurements at low carrier densities gave widths much smaller than the geometrical width. In addition, the widths deduced from the negative magnetoresistance region and the behaviour of the oscillation amplitude are about half of the geometrical width in this sample. This can be explained by enhanced scattering due to roughness of the lower interface of the QW, especially near the slopes of the groove.

In summary, quasi-one-dimensional quantum wires have been fabricated in V-grooves on GaAs substrates. Device geometries that enable formation of ohmic contacts outside the wires with relatively low series resistance were developed. Two-terminal magnetoresistance measurements of single-wire devices, using illumination as a carrier density modulator, show transport qualities not previously witnessed in growth on non-planar substrates. The illumination changed the lateral potential profile of the wires and characteristics were observed that were unique to different growth structures.

Acknowledgments

This work has been supported in part by the Basic Research Foundation administered by the Israeli Academy of Science and Humanities and by the Ministry of Defense.

References

[1] Kapon E, Hwang D M and Bhat R 1989 *Phys. Rev. Lett.* **63** 430
[2] Kapon E 1992 *Proc. IEEE* **80** 398
[3] Pfeiffer L, Stormer H L, Baldwin K W, West K W, Goni A R, Pinczuk A, Ashoori R C, Dignam M M and Wegscheider W J 1993 *J. Crystal Growth* **127** 849
[4] Wegscheider W, Kang W, Pfeiffer L N, West K W, Stormer H L and Baldwin K W 1994 *Solid-State Electron.* **37** 547
[5] Akiyama H, Someya T and Sakaki H 1996 *Phys. Rev.* B **53** R4229
[6] Yacoby A, Stormer H L, Baldwin K W, Pfeiffer L N and West K W *Solid-State Electron.* at press
[7] Honda T, Tarucha S, Saku T and Tokura Y 1995 *Japan. J. Appl. Phys.* **34** L72
[8] Mirin R P, Krishnamurthy M I-H, Bowers J E, Gossard A C and Hu E L 1992 *J. Vac. Sci. Technol.* A **10** 697
[9] Rinaldi R, Ferrara M, Cingolani R, Marti U, Martin D, Morier-Gemoud F, Ruterana P and Reinhart F K 1994 *Phys. Rev.* B **50** 11 795
[10] Warren A C, Woodal J M, Fossum E R, Pettit G D, Kirchner P D and McInturff D T 1987 *Appl. Phys. Lett.* **51** 1818
[11] Chabasseur-Molyneux V, Frost J E F, Simmons M Y, Ritchie D A and Pepper M 1996 *Appl. Phys. Lett.* **68** 3434
[12] Ballingall J M and Wood C E C 1982 *Appl. Phys. Lett.* **41** 947
[13] Miller D L and Asbeck P M J 1987 *J. Crystal Growth* **81** 368
[14] Harbury H K, Porod W and Goodnick S M 1993 *J. Appl. Phys.* **73** 1509
[15] Beenakker C W J and van Houten H 1991 *Solid State Phys.* vol 44, ed H Ehrenreich and D Turnbull (San Diego, CA: Academic) p 1